

Observation of $X(3872) \rightarrow J/\psi\gamma$ and Search for $X(3872) \rightarrow \psi'\gamma$ in B Decays

V. Bhardwaj,³⁹ K. Trabelsi,⁸ J. B. Singh,³⁹ S.-K. Choi,⁵ S. L. Olsen,^{42,7} I. Adachi,⁸ K. Adamczyk,³² D. M. Asner,³⁸ V. Aulchenko,^{1,36} T. Aushev,¹⁶ T. Aziz,⁴⁵ A. M. Bakich,⁴⁴ E. Barberio,²⁷ K. Belous,¹⁴ B. Bhuyan,⁹ M. Bischofberger,²⁹ A. Bondar,^{1,36} M. Bračko,^{25,17} J. Brodzicka,³² T. E. Browder,⁷ A. Chen,³⁰ P. Chen,³¹ B. G. Cheon,⁶ K. Cho,²⁰ Y. Choi,⁴³ J. Dalseno,^{26,46} Z. Doležal,² S. Eidelman,^{1,36} D. Epifanov,^{1,36} V. Gaur,⁴⁵ N. Gabyshev,^{1,36} B. Golob,^{24,17} J. Haba,⁸ K. Hayasaka,²⁸ H. Hayashii,²⁹ Y. Horii,⁴⁸ Y. Hoshi,⁴⁷ W.-S. Hou,³¹ Y. B. Hsiung,³¹ H. J. Hyun,²² T. Iijima,²⁸ K. Inami,²⁸ A. Ishikawa,⁴⁸ M. Iwabuchi,⁵⁵ Y. Iwasaki,⁸ T. Iwashita,²⁹ N. J. Joshi,⁴⁵ T. Julius,²⁷ J. H. Kang,⁵⁵ T. Kawasaki,³⁴ C. Kiesling,²⁶ H. O. Kim,²² J. B. Kim,²¹ J. H. Kim,²⁰ K. T. Kim,²¹ M. J. Kim,²² S. K. Kim,⁴² Y. J. Kim,²⁰ K. Kinoshita,³ B. R. Ko,²¹ N. Kobayashi,^{40,50} S. Korpar,^{25,17} P. Križan,^{24,17} R. Kumar,³⁹ T. Kumita,⁵¹ A. Kuzmin,^{1,36} Y.-J. Kwon,⁵⁵ J. S. Lange,⁴ M. J. Lee,⁴² S.-H. Lee,²¹ Y. Li,⁵³ J. Libby,¹⁰ C.-L. Lim,⁵⁵ D. Liventsev,¹⁶ R. Louvot,²³ D. Matvienko,^{1,36} S. McOnie,⁴⁴ K. Miyabayashi,²⁹ H. Miyata,³⁴ Y. Miyazaki,²⁸ R. Mizuk,¹⁶ G. B. Mohanty,⁴⁵ R. Mussa,¹⁵ E. Nakano,³⁷ M. Nakao,⁸ H. Nakazawa,³⁰ Z. Natkaniec,³² C. Ng,⁴⁹ S. Nishida,⁸ O. Nitoh,⁵² T. Nozaki,⁸ T. Ohshima,²⁸ S. Okuno,¹⁸ Y. Onuki,⁴⁸ G. Pakhlova,¹⁶ C. W. Park,⁴³ H. K. Park,²² R. Pestotnik,¹⁷ M. Petrič,¹⁷ L. E. Piilonen,⁵³ M. Röhrken,¹⁹ H. Sahoo,⁷ K. Sakai,⁸ Y. Sakai,⁸ T. Sanuki,⁴⁸ O. Schneider,²³ C. Schwanda,¹³ O. Seon,²⁸ M. Shapkin,¹⁴ V. Shebalin,^{1,36} T.-A. Shibata,^{40,50} J.-G. Shiu,³¹ B. Shwartz,^{1,36} P. Smerkol,¹⁷ Y.-S. Sohn,⁵⁵ A. Sokolov,¹⁴ E. Solovieva,¹⁶ S. Stanič,³⁵ M. Starič,¹⁷ T. Sumiyoshi,⁵¹ G. Tatishvili,³⁸ Y. Teramoto,³⁷ M. Uchida,^{40,50} S. Uehara,⁸ T. Uglov,¹⁶ Y. Unno,⁶ S. Uno,⁸ Y. Usov,^{1,36} G. Varner,⁷ A. Vossen,¹¹ X. L. Wang,¹² M. Watanabe,³⁴ Y. Watanabe,¹⁸ K. M. Williams,⁵³ B. D. Yabsley,⁴⁴ Y. Yamashita,³³ C. Z. Yuan,¹² C. C. Zhang,¹² Z. P. Zhang,⁴¹ V. Zhilich,^{1,36} P. Zhou,⁵⁴ V. Zhulanov,^{1,36} and A. Zupanc¹⁹

(Belle Collaboration)

¹*Budker Institute of Nuclear Physics, Novosibirsk*

²*Faculty of Mathematics and Physics, Charles University, Prague*

³*University of Cincinnati, Cincinnati, Ohio 45221*

⁴*Justus-Liebig-Universität Gießen, Gießen*

⁵*Gyeongsang National University, Chinju*

⁶*Hanyang University, Seoul*

⁷*University of Hawaii, Honolulu, Hawaii 96822*

⁸*High Energy Accelerator Research Organization (KEK), Tsukuba*

⁹*Indian Institute of Technology Guwahati, Guwahati*

¹⁰*Indian Institute of Technology Madras, Madras*

¹¹*Indiana University, Bloomington, Indiana 47408*

¹²*Institute of High Energy Physics, Chinese Academy of Sciences, Beijing*

¹³*Institute of High Energy Physics, Vienna*

¹⁴*Institute of High Energy Physics, Protvino*

¹⁵*INFN-Sezione di Torino, Torino*

¹⁶*Institute for Theoretical and Experimental Physics, Moscow*

¹⁷*J. Stefan Institute, Ljubljana*

¹⁸*Kanagawa University, Yokohama*

¹⁹*Institut für Experimentelle Kernphysik, Karlsruhe Institut für Technologie, Karlsruhe*

²⁰*Korea Institute of Science and Technology Information, Daejeon*

²¹*Korea University, Seoul*

²²*Kyungpook National University, Taegu*

²³*École Polytechnique Fédérale de Lausanne (EPFL), Lausanne*

²⁴*Faculty of Mathematics and Physics, University of Ljubljana, Ljubljana*

²⁵*University of Maribor, Maribor*

²⁶*Max-Planck-Institut für Physik, München*

²⁷*University of Melbourne, School of Physics, Victoria 3010*

²⁸*Nagoya University, Nagoya*

²⁹*Nara Women's University, Nara*

³⁰*National Central University, Chung-li*

³¹*Department of Physics, National Taiwan University, Taipei*

³²*H. Niewodniczanski Institute of Nuclear Physics, Krakow*

³³*Nippon Dental University, Niigata*

³⁴*Niigata University, Niigata*

- ³⁵University of Nova Gorica, Nova Gorica
³⁶Novosibirsk State University, Novosibirsk
³⁷Osaka City University, Osaka
³⁸Pacific Northwest National Laboratory, Richland, Washington 99352
³⁹Panjab University, Chandigarh
⁴⁰Research Center for Nuclear Physics, Osaka
⁴¹University of Science and Technology of China, Hefei
⁴²Seoul National University, Seoul
⁴³Sungkyunkwan University, Suwon
⁴⁴School of Physics, University of Sydney, New South Wales 2006
⁴⁵Tata Institute of Fundamental Research, Mumbai
⁴⁶Excellence Cluster Universe, Technische Universität München, Garching
⁴⁷Tohoku Gakuin University, Tagajo
⁴⁸Tohoku University, Sendai
⁴⁹Department of Physics, University of Tokyo, Tokyo
⁵⁰Tokyo Institute of Technology, Tokyo
⁵¹Tokyo Metropolitan University, Tokyo
⁵²Tokyo University of Agriculture and Technology, Tokyo
⁵³CNP, Virginia Polytechnic Institute and State University, Blacksburg, Virginia 24061
⁵⁴Wayne State University, Detroit, Michigan 48202
⁵⁵Yonsei University, Seoul
- (Received 2 May 2011; published 26 August 2011)

We report a study of $B \rightarrow (J/\psi\gamma)K$ and $B \rightarrow (\psi'\gamma)K$ decay modes using $772 \times 10^6 B\bar{B}$ events collected at the $Y(4S)$ resonance with the Belle detector at the KEKB energy-asymmetric e^+e^- collider. We observe $X(3872) \rightarrow J/\psi\gamma$ and report the first evidence for $\chi_{c2} \rightarrow J/\psi\gamma$ in $B \rightarrow (X_{c\bar{c}}\gamma)K$ decays, while in a search for $X(3872) \rightarrow \psi'\gamma$ no significant signal is found. We measure the branching fractions, $\mathcal{B}(B^\pm \rightarrow X(3872)K^\pm)\mathcal{B}(X(3872) \rightarrow J/\psi\gamma) = (1.78_{-0.44}^{+0.48} \pm 0.12) \times 10^{-6}$, $\mathcal{B}(B^\pm \rightarrow \chi_{c2}K^\pm) = (1.11_{-0.34}^{+0.36} \pm 0.09) \times 10^{-5}$, $\mathcal{B}(B^\pm \rightarrow X(3872)K^\pm)\mathcal{B}(X(3872) \rightarrow \psi'\gamma) < 3.45 \times 10^{-6}$ (upper limit at 90% C.L.), and also provide upper limits for other searches.

DOI: 10.1103/PhysRevLett.107.091803

PACS numbers: 13.20.Gd, 13.20.He, 14.40.Nd

The $X(3872)$ state was observed by the Belle Collaboration [1] in 2003, and later confirmed by CDF [2], D0 [3], and BABAR [4] Collaborations. The fact that it was not seen in decays to $\chi_{c1}\gamma$, $\chi_{c2}\gamma$, and $J/\psi\eta$ final states suggests that the $X(3872)$ is not a conventional $q\bar{q}$ meson state that can be explained by a simple quark model [1,5,6]. Because of its narrow width and the proximity of its mass, 3871.5 ± 0.2 MeV/ c^2 [7] to the $D^{*0}\bar{D}^0$ threshold, the $X(3872)$ is a good candidate for a $D\bar{D}^*$ molecule [11]. Other possibilities have also been proposed for the $X(3872)$ state, such as tetraquark [12], $c\bar{c}g$ hybrid meson [13], and vector glueball models [14].

Radiative decays of the $X(3872)$ are important in understanding its nature. One such decay, $X(3872) \rightarrow J/\psi\gamma$ [5,15], established its charge parity to be +1. In the molecular model, the radiative decays of the $X(3872)$ occur through vector meson dominance (VMD) and light quark annihilation (LQA) [11]. The decay rate of $X(3872) \rightarrow J/\psi\gamma$ is dominated by VMD while for $X(3872) \rightarrow \psi'\gamma$ [16] it is mostly driven by LQA, implying that $X(3872)$ decay to $\psi'\gamma$ is highly suppressed compared to $J/\psi\gamma$ [11]. Recent results from the BABAR Collaboration [17] show that $\mathcal{B}(X(3872) \rightarrow \psi'\gamma)$ is almost 3 times that of $\mathcal{B}(X(3872) \rightarrow J/\psi\gamma)$, which is inconsistent with a pure $D^{*0}\bar{D}^0$ molecular model, and can be interpreted as

indicating a $c\bar{c}-D^{*0}\bar{D}^0$ admixture [11,18]. If the $X(3872)$ is an admixture of χ'_{c1} and a molecular state, and its production and radiative decays are mainly due to its χ'_{c1} component, then the $\psi'\gamma$ decay, a favored $E1$ transition of χ'_{c1} , should be significantly enhanced compared to the $J/\psi\gamma$ decay, which is “hindered” by poor wave function overlap [19].

In this Letter, we present new results on $B \rightarrow (X_{c1}, X_{c2}, X(3872))K$, where the χ_{c1}, χ_{c2} decays to $J/\psi\gamma$ and the $X(3872)$ decays to $J/\psi\gamma$ or $\psi'\gamma$ [20]. These results are obtained from the final data sample of $772 \times 10^6 B\bar{B}$ events collected with the Belle detector [21] at the KEKB [22] energy-asymmetric e^+e^- collider operating at the $Y(4S)$ resonance. The Belle detector is a large-solid-angle spectrometer which includes a silicon vertex detector, a 50-layer central drift chamber (CDC), an array of aerogel threshold Cherenkov counters (ACC), time-of-flight scintillation counters (TOF), and an electromagnetic calorimeter (ECL) comprising CsI(Tl) crystals located inside a superconducting solenoid coil that provides a 1.5 T magnetic field.

The J/ψ meson is reconstructed in its decays to $\ell^+\ell^-$ ($\ell = e$ or μ), and the ψ' meson in its decays to $\ell^+\ell^-$ and $J/\psi\pi^+\pi^-$. In the $\psi' \rightarrow e^+e^-$ and $J/\psi \rightarrow e^+e^-$ decays, the four-momenta of all photons within 50 mrad of each of

the original e^+ or e^- tracks are included in the invariant mass calculation (hereafter denoted as $M_{e^+e^-(\gamma)}$), in order to reduce the radiative tail. The reconstructed invariant mass of the J/ψ candidates is required to satisfy $2.95 < M_{e^+e^-(\gamma)} < 3.13$ GeV/ c^2 or $3.03 < M_{\mu^+\mu^-} < 3.13$ GeV/ c^2 . In the $\psi' \rightarrow \ell^+\ell^-$ reconstruction, the invariant mass is restricted to the range $3.63 < M_{e^+e^-(\gamma)} < 3.72$ GeV/ c^2 or $3.65 < M_{\mu^+\mu^-} < 3.72$ GeV/ c^2 . To reconstruct $\psi' \rightarrow J/\psi \pi^+\pi^-$ decays, $\Delta M = M_{\ell^+\ell^-\pi^+\pi^-} - M_{\ell^+\ell^-}$ should satisfy the condition $0.58 < \Delta M < 0.60$ GeV/ c^2 . In order to reduce the combinatorial background due to low-momentum pions, the invariant mass of the two pions from the ψ' decay, $M_{\pi^+\pi^-}$, is required to be greater than 0.40 GeV/ c^2 . A mass- and vertex-constrained fit is performed to all the selected J/ψ and ψ' candidates to improve their momentum resolution.

The $\chi_{c1,c2}$ and the $X(3872)$ candidates are formed by combining the J/ψ candidates with a photon. Photons are reconstructed from clusters in the ECL and are required to have energies (in the lab frame) greater than 270 (470) MeV for $\chi_{c1,c2}$ [$X(3872)$] reconstruction. In a similar fashion, $X(3872)$ candidates decaying to $\psi'\gamma$ are reconstructed by combining ψ' candidates with γ candidates with energies greater than 100 MeV.

Charged tracks are identified as pion or kaon candidates using information from the CDC (dE/dx), TOF, and ACC systems. The kaon identification efficiency is 88%, while the probability of a pion misidentified as a kaon is 10%. The pions used in the reconstruction of the ψ' in the $J/\psi \pi^+\pi^-$ channel have an identification efficiency of 99% with a kaon to pion misidentification probability of 2%. Candidate K_S^0 mesons are reconstructed by combining two oppositely charged tracks (with a pion mass assumed) with invariant mass lying between [0.482, 0.514] GeV/ c^2 ; the selected candidates are required to satisfy the criteria given in detail in Ref. [23].

To reconstruct the B candidates, each $J/\psi\gamma$ or $\psi'\gamma$ system is combined with a kaon candidate. Two kinematic variables are formed: the beam-constrained mass ($M_{bc} \equiv \sqrt{E_{\text{beam}}^{*2} - p_B^{*2}}$) and the energy difference ($\Delta E \equiv E_B^* - E_{\text{beam}}^*$). Here E_{beam}^* is the run-dependent beam energy, and E_B^* and p_B^* are the reconstructed energy and momentum, respectively, of the B meson candidates in the $Y(4S)$ center-of-mass (c.m.) frame. Candidates having $M_{bc} > 5.27$ GeV/ c^2 and lying within a ΔE window of $[-25, 30]$ MeV for the $\chi_{c1,c2}$ and $[-30, 35]$ MeV ($[-20, 20]$ MeV) for $X(3872) \rightarrow J/\psi\gamma(X(3872) \rightarrow \psi'\gamma)$ are retained for further analysis. We extract the signal yield by performing an unbinned extended maximum likelihood fit to the variable $M_{\psi\gamma}$ defined as $M_{\ell\ell\gamma} - M_{\ell\ell} + m_\psi$ [24] or $M_{\ell\ell\pi\pi\gamma} - M_{\ell\ell\pi\pi} + m_{\psi'}$, where m_ψ or $m_{\psi'}$ is the world average mass [25]. In order to improve the resolution of $M_{\psi\gamma}$, we scale the energy of the γ so that ΔE is equal to zero.

To suppress continuum background, events having a ratio of the second to zeroth Fox-Wolfram moments [26] $R_2 > 0.5$ are rejected. Large $B \rightarrow \psi X$ Monte Carlo (MC) samples (corresponding to 50 times the data sample size used in this analysis) are used to study the background. To study the non- J/ψ (non- ψ') background $M_{\ell\ell}$ sidebands in data, within [2.5–2.6] GeV/ c^2 ([3.35–3.45] GeV/ c^2) and [3.2–3.5] GeV/ c^2 ([3.8–4.0] GeV/ c^2), are used.

For the $(J/\psi\gamma)K$ channels, the background is primarily from $B \rightarrow J/\psi K^*$ decays that do not peak in $M_{J/\psi\gamma}$. To reduce this background, we veto candidate photons from $\pi^0 \rightarrow \gamma\gamma$ by combining them with any other photon and then by rejecting both γ 's in the pair if the π^0 likelihood is greater than 0.52. This likelihood is a function of the laboratory energy of the other photon, its polar angle, and the invariant mass of the two-photon system, and is determined using MC study [27]. We also reject photon candidates with $\cos\theta_{\text{hel}} > 0.76$ (> 0.85) in the $\chi_{c1,c2}$ [$X(3872)$] selection, where the helicity angle θ_{hel} is defined as the angle between the direction of the photon and the direction opposite to the B momentum in the $\chi_{c1,c2}$ [$X(3872)$] rest frame. Applying these criteria, the background is reduced by 86% (79%) with a signal loss of 35% (30%) for the $B \rightarrow \chi_{c2}K$ [$B \rightarrow X(3872)K$] decay mode. For 1.3% of events with multiple candidates in $B \rightarrow (J/\psi\gamma)K$ decay modes, we select the B candidate having M_{bc} closest to the nominal B mass [25].

A sum of two Gaussians is used to model the signal shapes of $B \rightarrow \chi_{c1}K$ and $B \rightarrow \chi_{c2}K$. The fraction of each Gaussian is fixed to the value obtained from MC simulated events. For $B^+ \rightarrow \chi_{c1}K^+$ the other shape parameters are floated in the fit whereas for $B^+ \rightarrow \chi_{c2}K^+$ they are fixed using the mass difference (from Ref. [25]) and the width difference (from MC simulations) between the χ_{c1} and χ_{c2} . The nonpeaking combinatorial background component is modeled with a second-order polynomial. For the $B^0 \rightarrow \chi_{c1}K_S^0$ and $B^0 \rightarrow \chi_{c2}K_S^0$ decay modes, the signal shape is fixed using the results from the charged B mode.

Figure 1 shows the fit to the $M_{J/\psi\gamma}$ distribution for $B \rightarrow \chi_{c1}K$ and $B \rightarrow \chi_{c2}K$ decays in the range of [3.38, 3.70] GeV/ c^2 . We observe the χ_{c1} in both B decay modes, and obtain 3.6 standard deviation (σ) evidence for the χ_{c2} in the charged B decay mode. The branching fractions obtained in both cases are consistent with previous measurements [17,28]. The statistical significance is defined as $\sqrt{-2 \ln(\mathcal{L}_0/\mathcal{L}_{\text{max}})}$, where \mathcal{L}_{max} (\mathcal{L}_0) denotes the likelihood value when the yield is allowed to vary (is set to zero). Uncertainties in the probability density function (PDF) (the mean difference and width ratio) are estimated along with other systematic uncertainties (described below) and all are included in the significance [29]. As no significant signal is found for $B^0 \rightarrow \chi_{c2}K^0$, we determine a 90% C.L. upper limit (U.L.) on its branching fraction with a frequentist method that uses ensembles of pseudoexperiments. For a given signal yield, 10 000 sets of signal and

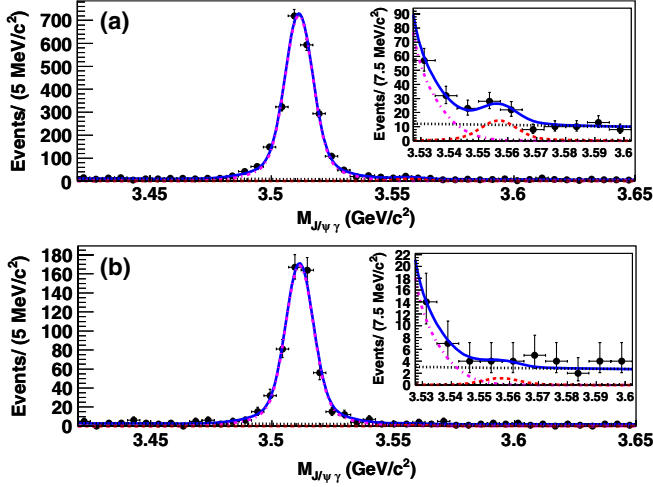


FIG. 1 (color online). $M_{J/\psi\gamma}$ distributions for (a) $B^+ \rightarrow \chi_{c1,c2}(\rightarrow J/\psi\gamma)K^+$ and (b) $B^0 \rightarrow \chi_{c1,c2}(\rightarrow J/\psi\gamma)K_S^0$ decays. The curves show the signal (pink dot-dashed for χ_{c1} and red dashed for χ_{c2}), and the background component (black dotted) as well as the overall fit (blue solid). The insets show a reduced range of $M_{J/\psi\gamma}$ and the contribution of the $B \rightarrow \chi_{c2}K$ peak.

background events are generated according to their PDFs, and fits are performed. The U.L. is determined from the fraction of samples that give a yield larger than that of data.

For the $B \rightarrow X(3872)(\rightarrow J/\psi\gamma)K$ decay mode, a sum of two Gaussians is also used to model the signal PDF, and the combinatorial background component is modeled by a first-order polynomial. To take into account small differences between the MC simulation and the data, the signal PDF shapes are corrected for calibration factors determined from the $B^+ \rightarrow \chi_{c1}K^+$ fit. Figure 2 shows the fit to the $M_{J/\psi\gamma}$ distributions for $B \rightarrow X(3872)K$ performed in the range $[3.7, 4.1]$ GeV/c^2 . We find a clear signal for $X(3872) \rightarrow J/\psi\gamma$ in the charged decay $B^+ \rightarrow X(3872)K^+$ with a significance of 4.9σ and measure the product branching fraction $\mathcal{B}(B^+ \rightarrow X(3872)K^+) \mathcal{B}(X(3872) \rightarrow J/\psi\gamma) = [1.78_{-0.44}^{+0.48}(\text{stat}) \pm 0.12(\text{syst})] \times 10^{-6}$. We also give an

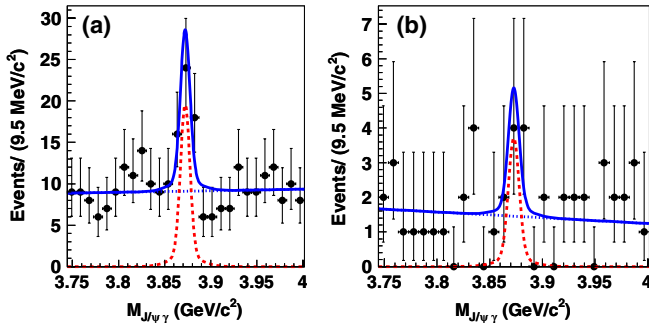


FIG. 2 (color online). $M_{J/\psi\gamma}$ distributions for (a) $B^+ \rightarrow X(3872)(\rightarrow J/\psi\gamma)K^+$ and (b) $B^0 \rightarrow X(3872)(\rightarrow J/\psi\gamma)K_S^0$ decays. The curves show the signal (red dashed) and the background component (blue dotted) as well as the overall fit (blue solid).

U.L. on the branching fraction for the neutral B mode whose significance is 2.4σ (Table I). Our results for $X(3872) \rightarrow J/\psi\gamma$ are consistent with previous results [5,17]. We estimate the significance of the $X(3872) \rightarrow J/\psi\gamma$ signal by simultaneously fitting the charged and the neutral B decay modes; we obtain a significance of 5.5σ including systematics uncertainties.

For the $B \rightarrow (\psi'\gamma)K$ decay mode, the background has a broad peaking structure, most of which is from $B \rightarrow \psi'K^*$ decay mode. Here, since the γ 's from $X(3872) \rightarrow \psi'\gamma$ have low energy [less than one third of the energy of the γ 's coming from $X(3872) \rightarrow J/\psi\gamma$], the π^0 -veto and $\cos\theta_{\text{hel}}$ selection result in more signal loss than background reduction. Instead, we combine the $\psi'K$ of the $\psi'\gamma K$ candidates with any π^\pm or π^0 candidate in the event. Three variables, namely, $\Delta E'$ ($\equiv E_{\psi'}^* + E_{K^*}^* - E_{\text{beam}}^*$),

$M'_{\text{bc}} [\equiv \sqrt{E_{\text{beam}}^{*2} - (p_{\psi'}^* + p_{K^*}^*)^2}]$, and the invariant mass of $K\pi$ ($M_{K\pi}$), are used for this purpose. Events satisfying the criteria of $817 < M_{K\pi} < 967$ MeV/c^2 , $\Delta E'$ within $[-20, 20]$ MeV and $M'_{\text{bc}} > 5.27$ GeV/c^2 , are identified as $B \rightarrow \psi'K^*$ candidates and discarded. This results in the reduction of the background by 59% with a 22% loss of signal. For 15.4% of events with multiple candidates in $B \rightarrow (\psi'\gamma)K$ decay modes, we select the B candidate having M_{bc} closest to the nominal B mass [25].

The branching fraction for the $B \rightarrow (\psi'\gamma)K$ mode is determined from a simultaneous fit performed to the two decay modes of the ψ' . The background shape for $B \rightarrow (\psi'\gamma)K$ has both a peaking and a nonpeaking component. For the peaking component, the shape is estimated from a large sample of MC simulated events of $\psi'K$ and $\psi'K^*$, and their fractions are fixed using the branching fractions from Ref. [25]. The nonpeaking background (combinatorial background) is parametrized by a threshold function $(M_{\psi'\gamma})^2 \exp[a(M_{\psi'\gamma} - M_{\text{th}}) + b(M_{\psi'\gamma} - M_{\text{th}})^2]$, where $M_{\text{th}} = 3.725$ GeV/c^2 . The ψ mass data sidebands and large $B \rightarrow \psi X$ MC sample (after removing $B \rightarrow \psi'X$ and $B \rightarrow \psi'X^*$ decays) are used to estimate the parameters of the threshold function. The shapes for both background components are fixed whereas their yields are allowed to float in the fit. The signal is described as a sum of two Gaussians and is fixed from MC study after applying calibration corrections (obtained from a study of $B^+ \rightarrow \chi_{c1}K^+$ data) while its yield is allowed to vary in the fit. No significant bias is found in fitting ensembles of the simulated experiments containing the signal and background components.

Figure 3 shows the results of the fit to the $M_{\psi'\gamma}$ distribution for $B \rightarrow X(3872)K$. The fitted yields are $5.0_{-11.0}^{+11.9}$ events ($1.5_{-3.9}^{+4.8}$ events) for $B^+ \rightarrow X(3872)K^+$ [$B^0 \rightarrow X(3872)K_S^0$]. Since there is no significant signal in either channel, we determine upper limits of $\mathcal{B}(B^+ \rightarrow X(3872)K^+) \times \mathcal{B}(X(3872) \rightarrow \psi'\gamma)$ [$\mathcal{B}(B^0 \rightarrow X(3872)K^0) \mathcal{B}(X(3872) \rightarrow \psi'\gamma)$] as 3.45×10^{-6} (6.62×10^{-6}) using the method

TABLE I. Corrected efficiency (ϵ), signal yield (Y) from the fit, measured \mathcal{B} or 90% C.L. upper limit (U.L.) for $B \rightarrow \chi_{c1,c2}K$, $B \rightarrow X(3872)(\rightarrow J/\psi\gamma)K$, and $B \rightarrow X(3872)(\rightarrow \psi'\gamma)K$ decay modes and significance (\mathcal{S}) with systematics included. \mathcal{B} for $B \rightarrow X(3872)K$ is the product $\mathcal{B}(B \rightarrow X(3872)K)\mathcal{B}(X(3872) \rightarrow \psi\gamma)$. For \mathcal{B} , the first (second) error is statistical (systematic).

Decay	ϵ (%)	Yield (Y)	Branching fraction	$\mathcal{S}(\sigma)$
$B \rightarrow \chi_{c1}(\rightarrow J/\psi\gamma)K$			$\mathcal{B} (\times 10^{-4})$	
K^+	14.8	2308^{+53}_{-52}	$4.94 \pm 0.11 \pm 0.33$	79
K^0	13.2	542 ± 24	$3.78^{+0.17}_{-0.16} \pm 0.33$	37
$B \rightarrow \chi_{c2}(\rightarrow J/\psi\gamma)K$			$\mathcal{B} (\times 10^{-5})$	
K^+	16.6	$32.8^{+10.9}_{-10.2}$	$1.11^{+0.36}_{-0.34} \pm 0.09$	3.6
K^0	14.4	$2.8^{+4.7}_{-3.9}$	$0.32^{+0.53}_{-0.44} \pm 0.03 (< 1.5)$	0.7
$B \rightarrow X(3872)(\rightarrow J/\psi\gamma)K$			$\mathcal{B} (\times 10^{-6})$	
K^+	18.3	$30.0^{+8.2}_{-7.4}$	$1.78^{+0.48}_{-0.44} \pm 0.12$	4.9
K^0	14.5	$5.7^{+3.5}_{-2.8}$	$1.24^{+0.76}_{-0.61} \pm 0.11 (< 2.4)$	2.4
$B \rightarrow X(3872)(\rightarrow \psi'\gamma)K$			$\mathcal{B} (\times 10^{-6})$	
K^+	14.7	$5.0^{+11.9}_{-11.0}$	$0.83^{+1.98}_{-1.83} \pm 0.44 (< 3.45)$	0.4
K^0	10.8	$1.5^{+4.8}_{-3.9}$	$1.12^{+3.57}_{-2.90} \pm 0.57 (< 6.62)$	0.3

described above. A completely independent analysis, with different selection criteria and a different fitting technique, was performed on the same data sample [30]; the results were found to be consistent with the results reported in this Letter.

The branching fractions and the fit results are summarized in Table I. Equal production of neutral and charged B meson pairs in the $Y(4S)$ decay is assumed. Secondary branching fractions used to calculate \mathcal{B} are taken from Ref. [25].

A correction for small differences in the signal detection efficiency calculated from the signal MC simulation and the data has been applied for the lepton (kaon or pion) identification requirement. Samples of $J/\psi \rightarrow \ell^+ \ell^-$ and $D^{*+} \rightarrow D^0(K^- \pi^+) \pi^+$ decays are used to estimate the lepton identification correction and the kaon (pion) identification correction, respectively. The uncertainties on these

corrections are included in the systematic error. The errors on the PDF shapes are obtained by varying all fixed parameters by $\pm 1\sigma$ and taking the change in the yield as the systematic error. To estimate the uncertainty arising from the fixed fractions of $B \rightarrow \psi'K$ and $B \rightarrow \psi'K^*$ in the $B \rightarrow (\psi'\gamma)K$ background shape, we vary their branching fractions by $\pm 1\sigma$. The uncertainty due to the secondary branching fractions are similarly taken into account. The uncertainty on the tracking efficiency and the number of recorded B meson pairs are estimated to be 1.0% per track and 1.4%, respectively. The uncertainty on the photon identification is estimated to be 2.0% and 3.0% for $B \rightarrow (J/\psi\gamma)K$ and $B \rightarrow (\psi'\gamma)K$, respectively. There is some possible efficiency difference of the selections (E_γ , π^0 veto, and $\cos\theta_{\text{hel}}$) between the data and the MC calculations. This difference in the $B \rightarrow (J/\psi\gamma)K$ study is estimated to be 3.0% using the $B^+ \rightarrow \chi_{c1}K^+$ sample. Because of the nonavailability of a proper model to generate χ_{c2} in the EVTGEN simulation [31], and the ambiguity in the allowed $X(3872)$ J^{PC} values (1^{++} or 2^{-+}) [32], we generate χ_{c2} and $X(3872)$ assuming them to be scalar, vector, and tensor particles. We find that 4.0% is the maximum possible difference in the efficiency and include it in the systematic error.

In summary, we observe $X(3872) \rightarrow J/\psi\gamma$ in B decays and present the most precise measurement to date of the product branching fraction $\mathcal{B}(B^+ \rightarrow X(3872)K^+) \times \mathcal{B}(X(3872) \rightarrow J/\psi\gamma) = (1.78^{+0.48}_{-0.44} \pm 0.12) \times 10^{-6}$. We also report evidence for $B \rightarrow \chi_{c2}K$, and the ratio of $\mathcal{B}(B^+ \rightarrow \chi_{c2}K^+)/\mathcal{B}(B^+ \rightarrow \chi_{c1}K^+)$ is measured to be $(2.25^{+0.73}_{-0.69} \pm 0.17)\%$. The measured branching fraction of $B \rightarrow \chi_{c2}K$ is even more suppressed than expected compared to a recent theoretical prediction [33]. We find no evidence for $X(3872) \rightarrow \psi'\gamma$ and give an U.L. on its

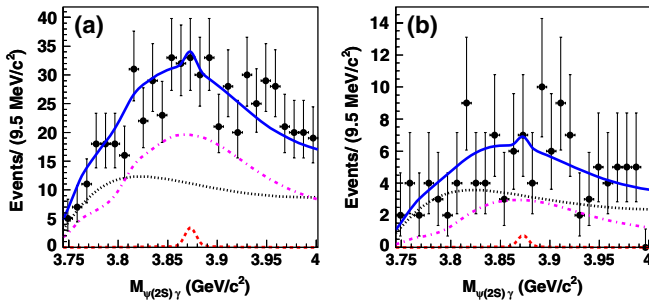


FIG. 3 (color online). $M_{\psi'\gamma}$ distributions for (a) $B^+ \rightarrow X(3872)(\rightarrow \psi'\gamma)K^+$ and (b) $B^0 \rightarrow X(3872)(\rightarrow \psi'\gamma)K^0$. The curves show the signal [red dashed for $X(3872)$] and the background component [pink dot-dashed for background from $B \rightarrow \psi'K^*$ and $B \rightarrow \psi'K$ component, and black dotted for combinatorial background modeled by the threshold function] as well as the overall fit (blue solid).

branching fraction as well as the following limit $R(\equiv \frac{\mathcal{B}(X(3872) \rightarrow \psi' \gamma)}{\mathcal{B}(X(3872) \rightarrow J/\psi \gamma)}) < 2.1$ (at 90% C.L.). The $X(3872)$ state may not have a large $c\bar{c}$ admixture with a $D^{*0}\bar{D}^0$ molecular component as was expected on the basis of the BABAR Collaboration result [17].

We thank the KEKB group for excellent operation of the accelerator, the KEK cryogenics group for efficient solenoid operations, and the KEK computer group and the NII for valuable computing and SINET3 network support. We acknowledge support from MEXT, JSPS, and Nagoya's TLPRC (Japan); ARC and DIISR (Australia); NSFC (China); MSMT (Czechia); DST (India); MEST, NRF, NSDC of KISTI, and WCU (Korea); MNiSW (Poland); MES and RFAAE (Russia); ARRS (Slovenia); SNSF (Switzerland); NSC and MOE (Taiwan); and DOE (U.S.).

-
- [1] S. K. Choi *et al.* (Belle Collaboration), *Phys. Rev. Lett.* **91**, 262001 (2003).
- [2] D. Acosta *et al.* (CDF Collaboration), *Phys. Rev. Lett.* **93**, 072001 (2004).
- [3] V. M. Abazov *et al.* (D0 Collaboration), *Phys. Rev. Lett.* **93**, 162002 (2004).
- [4] B. Aubert *et al.* (BABAR Collaboration), *Phys. Rev. D* **71**, 071103 (2005).
- [5] K. Abe *et al.* (Belle Collaboration), arXiv:hep-ex/0408116.
- [6] B. Aubert *et al.* (BABAR Collaboration), *Phys. Rev. Lett.* **93**, 041801 (2004).
- [7] Our own average using the most recent measurements [$X(3872) \rightarrow J/\psi \pi\pi$ decay channel] from Belle, BABAR, CDF, and D0 Collaborations [3,8–10].
- [8] I. Adachi *et al.* (Belle Collaboration), arXiv:0809.1224.
- [9] B. Aubert *et al.* (BABAR Collaboration), *Phys. Rev. D* **77**, 111101 (2008).
- [10] T. Aaltonen *et al.* (CDF Collaboration), *Phys. Rev. Lett.* **103**, 152001 (2009).
- [11] E. S. Swanson, *Phys. Lett. B* **598**, 197 (2004); E. S. Swanson, *Phys. Rep.* **429**, 243 (2006).
- [12] L. Maiani *et al.*, *Phys. Rev. D* **71**, 014028 (2005).
- [13] B. A. Li, *Phys. Lett. B* **605**, 306 (2005).
- [14] K. K. Seth, *Phys. Lett. B* **612**, 1 (2005).
- [15] B. Aubert *et al.* (BABAR Collaboration), *Phys. Rev. D* **74**, 071101(R) (2006).
- [16] The ψ' , which is sometimes designated as the $\psi(2S)$, is not a pure S -wave vector charmonium, rather it has a significant admixture of 3D_1 : $|\psi'\rangle = \cos\phi|2{}^3S_1\rangle - \sin\phi|1{}^3D_1\rangle$.
- [17] B. Aubert *et al.* (BABAR Collaboration), *Phys. Rev. Lett.* **102**, 132001 (2009).
- [18] M. Suzuki, *Phys. Rev. D* **72**, 114013 (2005).
- [19] T. Barnes and S. Godfrey, *Phys. Rev. D* **69**, 054008 (2004).
- [20] Hereafter charge-conjugate and neutral modes are included throughout the Letter unless stated otherwise.
- [21] A. Abashian *et al.* (Belle Collaboration), *Nucl. Instrum. Methods Phys. Res., Sect. A* **479**, 117 (2002).
- [22] S. Kurokawa and E. Kikutani, *Nucl. Instrum. Methods Phys. Res., Sect. A* **499**, 1 (2003), and other papers included in this volume.
- [23] K-F. Chen *et al.* (Belle Collaboration), *Phys. Rev. D* **72**, 012004 (2005).
- [24] Here ψ refers to J/ψ or ψ' and $\psi\gamma$ refers to χ_{c1} , χ_{c2} , or $X(3872)$ depending upon the particle being reconstructed.
- [25] K. Nakamura *et al.* (Particle Data Group), *J. Phys. G* **37**, 075021 (2010).
- [26] G. C. Fox and S. Wolfram, *Phys. Rev. Lett.* **41**, 1581 (1978).
- [27] P. Koppenburg *et al.* (Belle Collaboration), *Phys. Rev. Lett.* **93**, 061803 (2004).
- [28] N. Soni *et al.* (Belle Collaboration), *Phys. Lett. B* **634**, 155 (2006).
- [29] R. D. Cousins and V. L. Highland, *Nucl. Instrum. Methods Phys. Res., Sect. A* **320**, 331 (1992).
- [30] The independent analysis uses a three-dimensional fit (M_{bc} , ΔE , and $M_{\psi'\gamma}$) to extract the signal yield. The mass of the reconstructed B (instead of ΔE) is used to scale E_γ in order to improve the resolution of $M_{\psi'\gamma}$.
- [31] D. J. Lange, *Nucl. Instrum. Methods Phys. Res., Sect. A* **462**, 152 (2001).
- [32] A. Abulencia *et al.* (CDF Collaboration), *Phys. Rev. Lett.* **98**, 132002 (2007).
- [33] M. Beneke and L. Vernazza, *Nucl. Phys.* **B811**, 155 (2009).